Powder Metallurgy (2014), 57(5), 357-364.
DOI: http://dx.doi.org/10.1179/1743290114Y.0000000119

Understanding contribution of microstructure to fracture behaviour of sintered steels

J. M. Torralba*[1,2], L. Esteban[1], E. Bernardo[1] and M. Campos[1]

[1] Department of Materials Science and Engineering, Universidad Carlos III de Madrid, Avd. de la Universidad 30, 28911 Leganés, Madrid, Spain
[2] IMDEA Materials Institute, C/Eric Kandel 2, Tecnogetafe, 28906 Getafe, Madrid, Spain
* Corresponding author, email j.torralba@imdea.org

Abstract: Microstructural features of sintered steels, which comprise both phases and porosity, strongly condition the mechanical behaviour of the material under service conditions. Many research activities have dealt with this relationship since better understanding of the microstructure–property correlation is the key of improvement of current powder metallurgy (PM) steels. Up to now, fractographic investigation after testing has been successfully applied for this purpose and, more recently, the *in situ* analysis of crack evolution through the microstructure as well as some advanced computer assisted tools. However, there is still a lack of information about local mechanical behaviour and strain distributions at the microscale in relation to the local microstructure of these steels, i.e. which phases in heterogeneous PM microstructures contribute to localisation of plastic deformation or which phases can impede crack propagation during loading. In the present work, these questions are addressed through the combination of three techniques: (i) *in situ* tensile testing (performed in the SEM) to monitor crack initiation and propagation; (ii) digital image correlation technique to trace the progress of local strain distributions during loading; (iii) fractographic examination of the loaded samples. Three PM steels, all obtained from commercially available powders but presenting different microstructures, are examined: a ferritic–pearlitic Fe–C steel, a bainitic prealloyed Fe–Mo–C steel and a diffusion alloyed Fe–Ni–Cu–Mo–C steel, with more heterogeneous microstructure (ferrite, pearlite, upper and lower bainite, martensite and Ni rich austenite).

Keywords: Sintered steels, Fracture, Crack growth, Microstructure–property relationship, *In situ* tensile testing, Digital image correlation

Introduction

Fracture behaviour of sintered steels has been widely investigated in the literature. In most of the works, the study is made using fatigue tests because through fatigue, the nucleation and propagation of a crack are the key point for understanding the fracture mode of the studied materials.[1–5] In all the works related to the fracture behaviour, it is highlighted that one of the main cause responsible for the nucleation and propagation of cracks is porosity. When an external load is applied, pores act as stress–concentrators and give rise to unbalanced strains within the metallic matrix. Porosity features such as size, shape, amount, connectivity and distance between adjacent pores have a high impact on properties. Regarding porosity, two important aspects can be highlighted: (i) at higher densities, more homogeneously distributed porosity can be reached, and smaller and more rounded pores,[6] and (ii) big and irregular pores induce the greatest damage in the mechanical properties, with special impact on the ductility of the steels.[7,8] In this sense, big secondary pores generated by transient liquid phase sintering can be especially detrimental.[9]

Once porosity has been defined as the main cause for crack initiation, preferential sites for crack growth and propagation should be identified. There are many studies where this matter has been studied through *post mortem* fracture observations, in particular heterogeneous steels obtained from diffusion bonded powders have attracted the major interest (under the point of view of the different microconstituents present at the microstructure).[1,10] Nevertheless, there are some studies in this sense concerning fully prealloyed high performance grades.[4,11]

Although most of the works in this field were based on fatigue tests, some studies based on *in situ* static tests can be found.[12,13] The unique approach to the use of plastic deformation maps to contribute to the understanding of the fracture behaviour in these family of steels was found using microhardness maps and correlating the brittleness of the present phases with the deformation behaviour of the full sample.[14] In Ref. 9, an interesting approach is made to the knowledge of the local plasticity linked with the microstructure through finite element analysis.

Therefore, if we try to summarise the main conclusions of all those works, we could highlight two main ideas. First, the main origin of the cracks in sintered steels under static or dynamic loads is the pores, the predominant path for the cracks propagation being the shorter distance between two critical pores. The porosity effect is much more important than the possible effect of the presence of different microconstitutents with different plasticity features. Second, once the crack is running through the microstructure, the main preferential path is the interface among microconstituents (pearlite/martensite, pearlite/austenite) more than across the middle of the pearlite, the austenite or the martensite.

One discussion that was established for many years is the role of the Ni rich (austenitic) areas that can be found in the steels obtained from diffusion alloyed powders. On the one side, in these areas, there are a high number of micropores (Kirkendall pores) capable of creating high stress level and inducing the origin of a crack. On the other side, it seems that austenite could stop the evolution of a crack path due to its high capability of deformation (and consuming this energy it is not used to nucleate or propagate cracks) and the capability of austenite to be transformed in martensite by plasticity, as pointed in Ref. 15. It is not really clear in the literature what is the role of these microstructural areas, being[8,9] against the theory of the positive effect of the austenite areas.

This work aims to contribute to the understanding of the microstructure–performance correlation through the combination of advanced techniques. The role of local microstructure on local mechanical behaviour and local strain distribution is examined using three different techniques: (i) *in situ* tensile test (inside the SEM), where the initiation of the crack and its propagation can be monitored (and where the crack path during the test can be seen); (ii) the digital image correlation (DIC) technique, which allows to identify which individual microconstituent is contributing in the plastic deformation process during loading; (iii) the study of the fracture surface of the samples after the static tensile test. In our work, we have also introduce a plain Fe–C steel in addition to other two steels obtained from fully prealloyed powders and diffusion bonded powders widely studied in the literature. In all the cases, the obtained materials reached the same level of density trying to avoid this variable in the analysis.

Experimental

For this study, three different sintered steels were obtained using different powder grades (all of them provided by Höganäs AB, Sweden). The chemical composition of each grade is shown in Table 1.

The Fe base powders were mixed with 0·7 wt-% natural graphite (UF4 grade, from Kropfmül, Germany) to reach, after sintering, ~0·55 wt-% of combined carbon. All materials were uniaxially pressed into discs of 16 mm diameter and sintered in a lab furnace to reach a similar level of density close to 7·25 g cm^{-3}, sintering was carried out in N_2-10 vol.-% H_2-0·1 vol.-% CH_4 atmosphere at 1150°C. Samples were cooled down in the furnace after sintering. The obtained sintered steels were tagged respectively as FeC, AstMo and diffusion alloyed steel (DAE). Before machining the mini tensile bars (according to Fig. 1), on the sintered samples, density (by Archimedes' method) and hardness HV30 were measured. Microstructural analysis was also performed to check the obtained microstructure.

Table 1 Chemical composition of used powder grades/ wt-%

Grade	Ni	Cu	Mo	Fe
ASC 100·29	…	…	…	Bal.
Astaloy Mo	…	…	1·5	Bal.
Distaloy AE	4·0	1·5	0·5	Bal

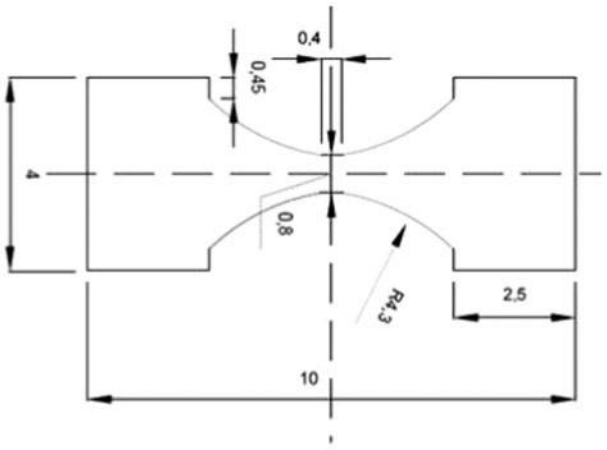

1 Sketch of tensile specimen geometry (dimensions are in millimetres; thickness: 1 mm

Micro dog bone tensile specimens with the dimensions shown in Fig. 1 were machined from the centre of the sintered discs, in perpendicular direction to the pressing direction. The central part of the sample gauge section was reduced to 0·8 mm in order to more easily identify sites of crack nucleation and propagation. The samples were grinded and polished (0·3 μm alumina). Tensile load was applied with a rate of 10^{-3} s^{-1} using a Kammrath&Weiss tensile compression module. *Ex situ* tests were used to measure the yield strength (YS), the ultimate tensile strength (UTS) and the elongation ε. For *in situ* testing, loading was carried out inside a Zeiss EVO MA15 SEM on etched samples (1% nital solution).

To analyse the origin and the crack propagation in the *in situ* tests, the application of the load was stopped at different levels of strain to have different images. In the case of the DIC analysis (explained bellow), all the images for the analysis were taken after releasing the load for the selected specific strains.

In DIC, we can obtain deformation maps associated with the different phases or microconstituents that are present in the microstructure. From the starting microstructure and taking as reference different points in the surface of the specimen, the displacement correlation in DIC is based on the movement of those key points, tracked and compared with the initial position. When the sample is submitted to a tensile stress, after certain level of strain, it can be tracked, by comparison, the plastic deformation level once the stress is relaxed and by comparison with the microstructure with the original one (through the displacement of the key points). The accuracy of the method will be related to two different parameters: the size of the key point (which can be from some micrometres to hundreds of micrometres in size)

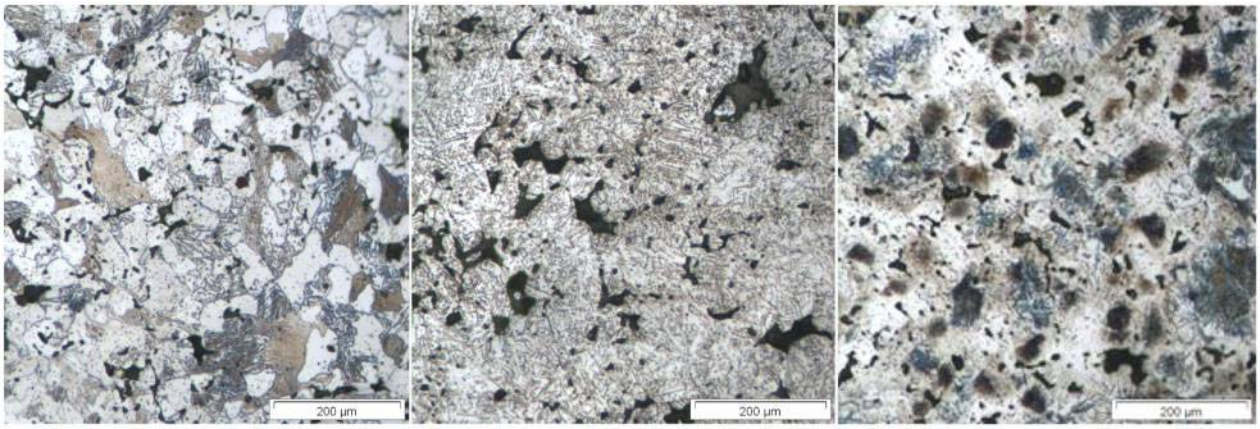

2 From left to right: FeC, Ast Mo and DAE

and the distance of the measured images to the place where fracture takes places at the end of the test (which can also be a few micrometres or more). In Ref. 16, the technical principles where DIC is based is explained. The study is completed with a fractographic analysis on the fresh fracture produced after a tensile test in each material, using SEM.

Results and discussion

Microstructure and mechanical properties of steels

Since this study deals with very well known materials, with regards to microstructure and macroscopic mechanical properties, the initial characterisation presented in Fig. 2 and Table 2 is used to confirm the expected results. Tensile values obtained from the special designed test specimens cannot be fully considered due to the specific dimensions of the samples, completely out of the standards, but they are shown to confirm, as well as the microstructures (Fig. 2) and the hardness values, that the obtained materials exhibit the expected features for the same materials with a similar level of density tested in standard conditions.

As a guideline, Table 2 also displayed values from the powder manufacturer, as similar levels of density, differences in cooling rate, sintering T and tensile bar geometry can lead to deviations. In Fig. 3, the engineering stress/strain curves for all the studied materials can be compared.

Study of crack initiation and propagation

In Fig. 4, the macroscopic evolution of the tensile test for the AstMo steel, being this figure completely representative of the behaviour of all the studied steels (including the FeC, which exhibits the highest plastic deformation before fracture takes place, as can be seen in Fig. 3, right) is shown. These materials break without any reduction in section, and once a crack is nucleated,

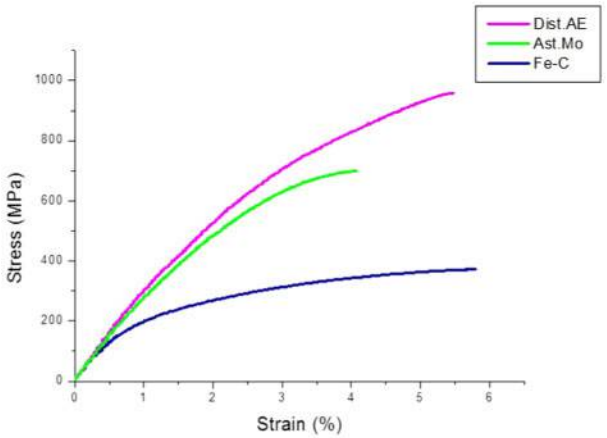

3 Comparative engineering stress/strain curves for all studied steels

propagation is very fast and fracture takes place close to the highly stressed area (the designed area).

Fracture of FeC sintered steel

In the Fe–C steel, first microcracks nucleate at 2–3% of strain (which represents the 30–50% of the total strain at failure) and are linked always with porosity. Big, elongated, sharp pores, perpendicularly orientated to the loading axis, are preferential sites for crack initiation. As loading progressively increases, nucleated cracks rapidly propagate to adjacent pores through the shortest distances between the pores, as can be seen in the upper image of Fig. 5. Fracture of these steels leads to high concentration of plastic deformation around the critical pores and at sinternecks. Localisation of plastic deformation is extremely high at pores surrounded by ferrite, and formation of slip lines is favoured at these places. These slips lines, when pores are relatively close together, start to sketch the future fracture path.

Table 2 Key properties of studied steels

Steel	Hardness/HV30	YS/MPa	UTS/MPa	ε/%	Hardness/HV30*	YS/MPa*	UTS/MPa*	ε/%*
FeC	139	240	409	5·8	125	220	350	6
AstMo	212	550	737	4·0	175	490	670	3
DAE	238	675	985	6·3	240	445	820	3·7

*From Höganäs AB handbooks.

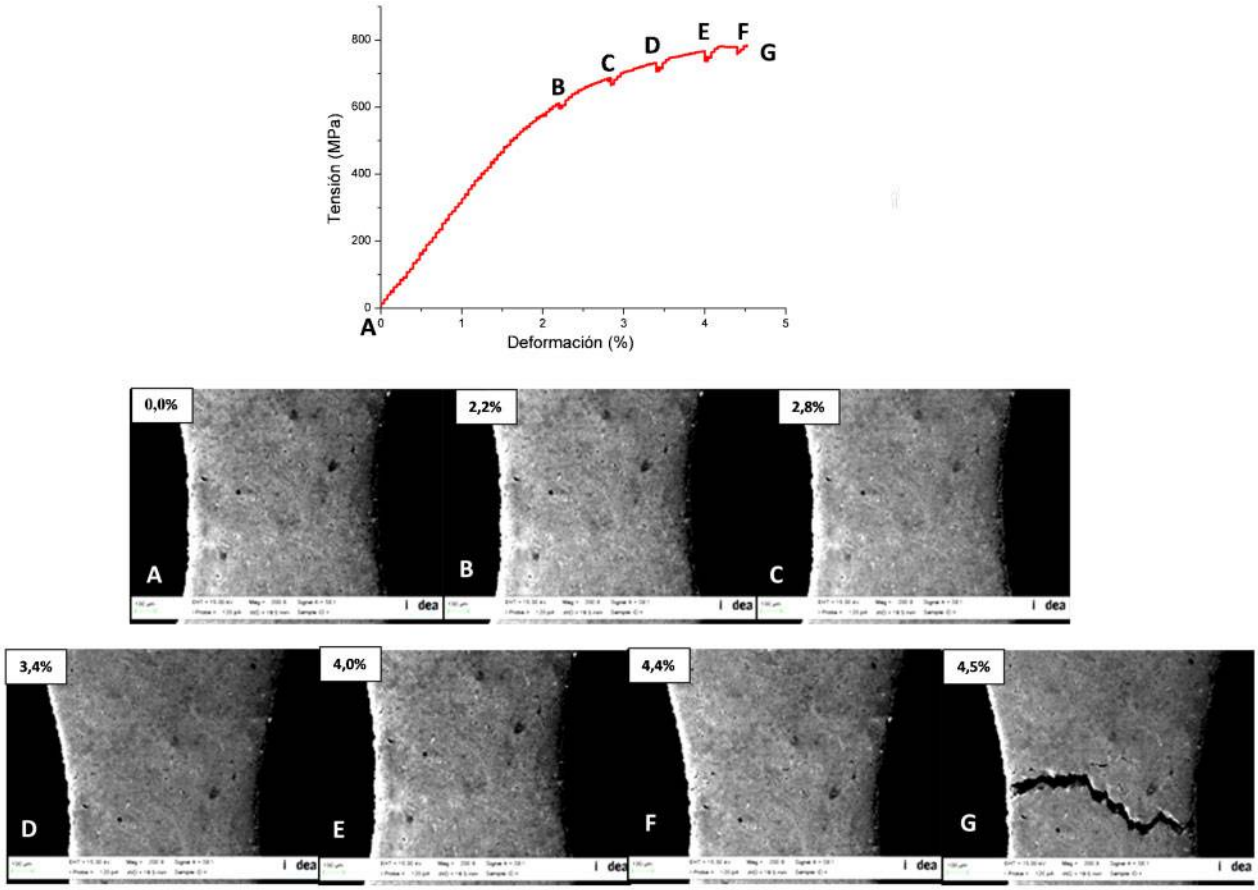

4 Macroscopic evolution of tensile *in situ* test for AstMo; micrographs are related with the tagged points in the tensile curve

When fracture takes place, the border of the fracture follows exactly the predicted path (compare the slips net created between the nearest pores in the upper part of Fig. 4, with the fracture line of the bottom part of the figure). The trajectory of the fracture from pore to pore always has a preferential way through the interface between ferrite and pearlite, and in some cases, the path can take the way through the pearlite, but always in the interface ferrite/cementite.

In Fig. 6, a model of this phenomenon is described, where we can distinguish the main preferential path of the crack (a) from pore to pore, and the alternative path (b) through the interface ferrite/cementite inside the pearlite. This model is fully confirmed through the analysis of the fracture surface.

Looking with more detail into the edge of the fracture line, elongated dimples produced by the deformation of the ferrite from pearlite (main resistant constituent in the steel) can be clearly seen (Fig. 7, left). In addition, in the ordinary fracture surface, typical dimples produced by fracture of the ferrite (plain ferrite or ferrite in the pearlite) can be seen as the main bearing cross-section (Fig. 7, right).

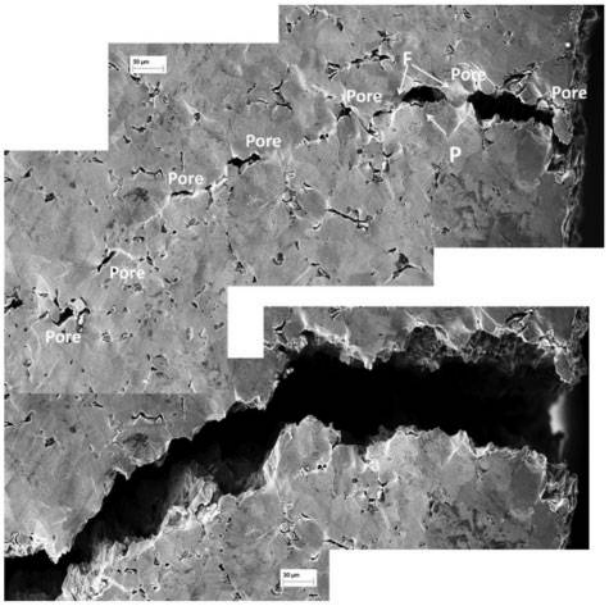

5 Fe–C steel fracture path, just before fracture and after breaking

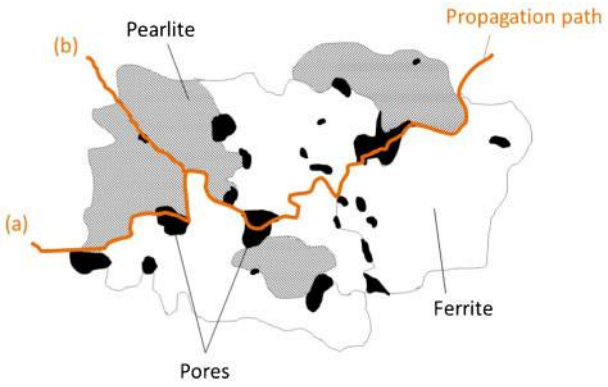

6 Crack propagation path through microstructure of FeC

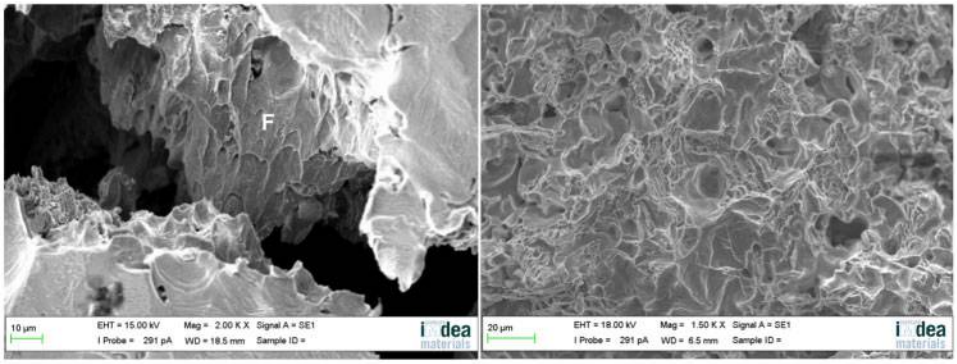

7 Fracture surface of FeC steel

Fracture of AstMo steel

In the AstMo steel, similar behaviour can be observed (Fig. 8), but with two main differences. Owing to the homogeneous microstructure, the fracture path goes between the grains of the bainite (instead the ferrite–pearlite microstructure of the plain carbon steels), and the level of deformation is much smaller, plasticity signs in the sharp corners of the pores being less evident (Fig. 9).

In Fig. 10, a model of the crack propagation path through the microstructure of the AstMo is presented, in accordance with the experimental results obtained.

In addition, the proposed model is fully confirmed with the fracture surface, which is mainly composed of dimples produced in the bainite (Fig. 11).

Fracture of DAE steel

In these steels, we have a completely heterogeneous microstructure with more than two microconstituents. Here, it is more difficult to understand the fracture behaviour because of the presence of martensitic areas linked with Ni rich austenitic areas usually concentrated in the border of the former particles. The role in the fracture behaviour of these austenitic areas has been a discussion topic in many papers in the literature. If we analyse the *in situ* images for these two steels, cracks are specially nucleating at the Kirkendall porosity associated with those areas. This fact is widely produced among all the microstructure as loading is increased, and once the crack is originated, it propagates very fast in the neighbour martensite, between the austenite and the pearlite. In Fig. 12, we can see some incipient cracks generated in the middle of these areas (top), and when load reaches a critical value, the final crack path travels by the brittle interface among the austenite and the other microconstituents (bottom).

If we analyse the crack path when fracture takes place (Fig. 13), it can be seen that the preferential path is the interface between the high alloyed microconstituents (linked to austenite and martensite) and the pearlite/bainite. This fact has been also reported by Ref. 10, how cracks are created near the interface pearlite/austenite and their growth and propagation among this interface are fully described and supplemented with a complete microstructural study. It is discussed that pores at the interface appear to be critical and act as crack initiation sites.

However, the question is whether retained austenite due to high Ni concentration is contributing to plastic deformation in support of the progress of the fracture path. According to some authors, when cracks arrive at an austenitic area, it tends to be stopped due to the absorption of the plastic energy by the austenite, which could be transformed in martensite.[13,17] In Ref. 10, it is also suggested that pores created inside the austenite, at least at the beginning and due to ductile character of the austenite, can reduce or delay their noxious effect. In our *in situ* test, we have two opposite effects promoted by the presence of the austenitic areas. On the one hand, if these austenitic areas are big, they could be considered as detrimental if they have associated large diffusion pores, where cracks can be easily nucleated. On the other hand, it can be found that many 'stopped' cracks inside the austenite, where the effect of the austenite as absorber of the energy is clearly seen (*see* Fig. 12). This means that the size of these areas could have an important role in the toughness of the steel. What is clear is that propagation of the cracks takes place at the interface of the rich alloying elements areas (where we have Ni rich austenite surrounded by Cu–Mo rich martensite) and poor alloying elements areas (where we have ferrite/pearlite). In these interfaces, the sintering

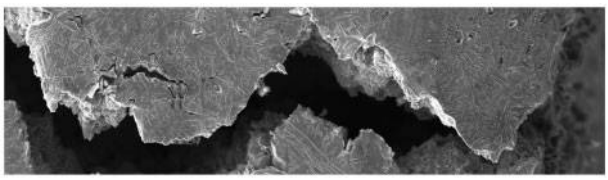

8 Astaloy Mo fracture path after breaking

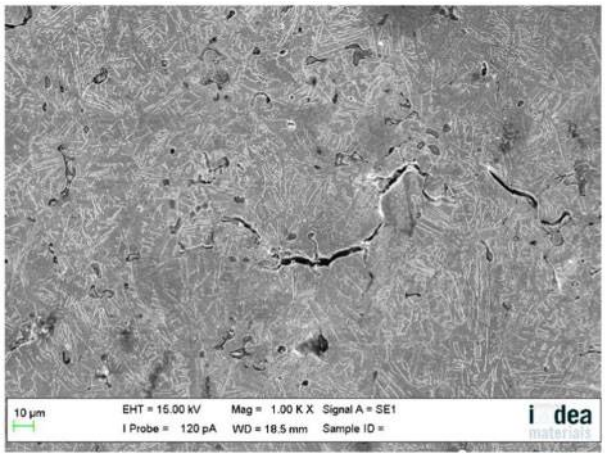

9 Initiated crack in Astaloy Mo before breaking

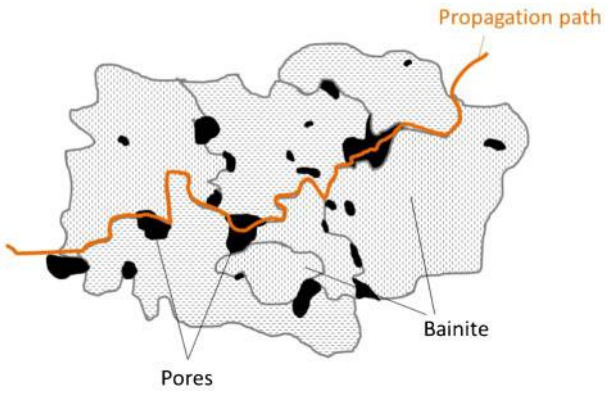

10 Model of crack propagation path through microstructure of AstMo

necks where the main part of the load is supported by the steels were established (see the fracture surface of Fig. 14). Here, we can see facets of cleavage associated to failure in austenite/martensite, without any plastic deformation, and dimples in the areas where pearlite/bainite is supporting part of the load.

In the case of the heterogeneous powder metallurgy steels (DAE), we can also try to model the crack propagation path, in accordance with all the obtained results. It is shown in Fig. 15. Here, in some critical points, the crack can follow the grain boundary through the brittle martensite [route (a) in Fig. 15], or cross through the pearlitic grains [route (b) in Fig. 15]. These two different possible paths would produce, in the fracture surface, cleavage (when the cross-section is martensite) or a mix of cleavage and dimples (when the cross-section moves into the pearlite, as can be seen in Fig. 14).

Evolution of local strain distribution

This analysis of the results is fully confirmed with the deformation maps obtained with DIC technique (Fig. 16). In the case of the Fe–C steel, we can find a certain level of plastic deformation when 51% of strain is reached and fully associated with areas where the critical pores have induced the nucleation of cracks. In the case of the AstMo, plastic deformation is detected at ~83% of the total strain at break and only a few parts of the microstructure are showing plastic deformation near the pores that are sites for cracks nucleation. Here, there is a random association of the plasticity with the microstructure because it is fully bainitic and maybe the unique tendency could be associated with the grain

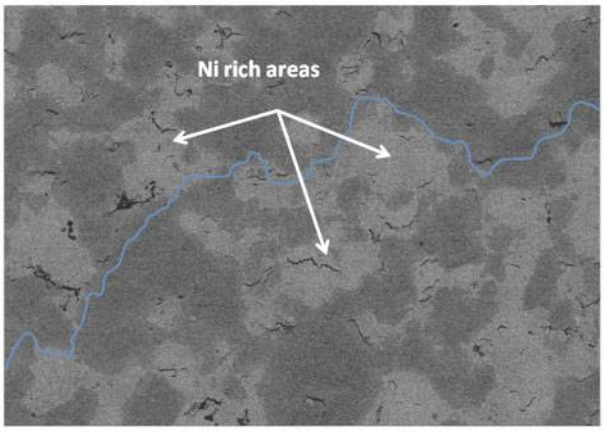

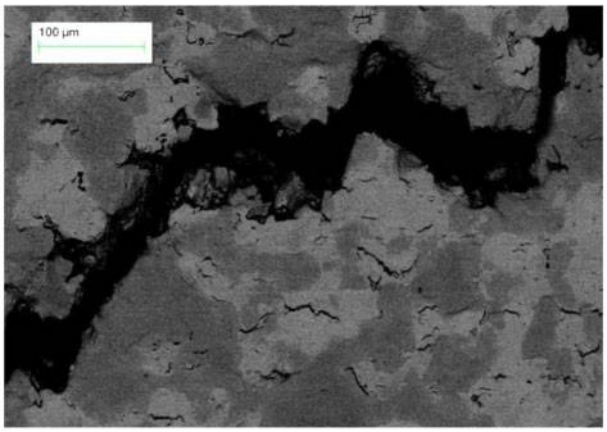

12 Crack nucleation in DAE under critical load

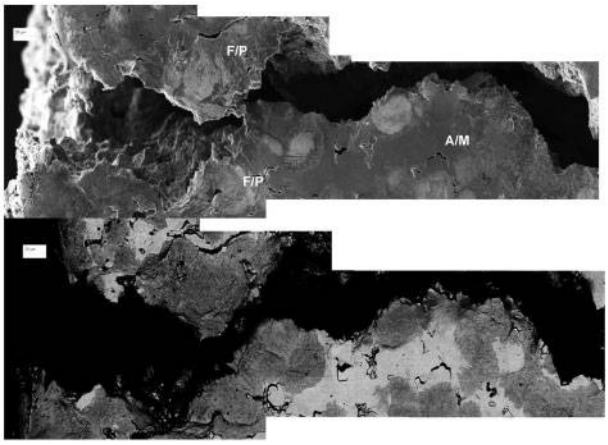

13 Fracture path in DAE. Up, secondary electrons image; down, back scattering electrons image

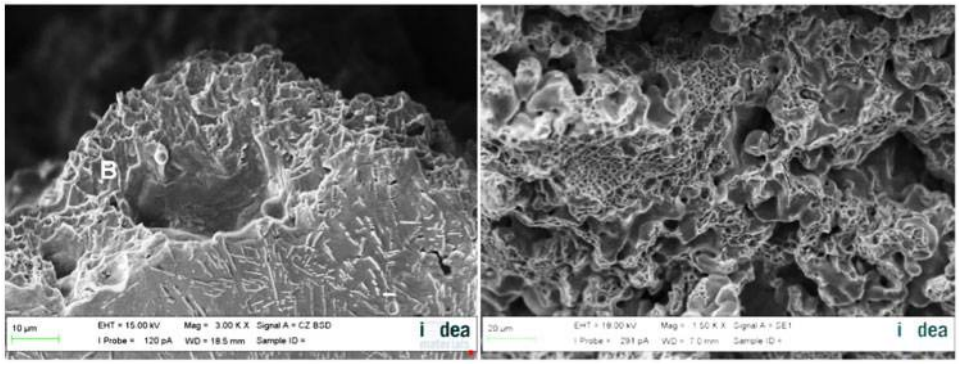

11 Fracture of Astaloy Mo steel

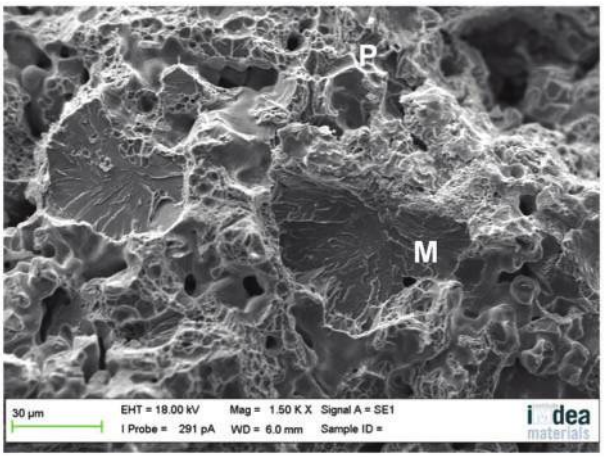

14 **Fracture surface of DAE**

15 **Model of crack propagation path through microstructure of DAE**

orientations. Chawla and Deng[7] present an interesting work of simulation by FEM, where deformation maps produced by simulation techniques show how the largest and interconnected pores can produce strain intensification, which is in total agreement with what can be seen in our *in situ* tests (Fig. 4) and with the phenomena described by the DIC deformation maps obtained from experimental results (Fig. 16).

If we analyse the DIC results for the DAE (Fig. 16), the level of the local plastic deformation at the austenitic areas is in the lower range of the measured plastic deformation. However, in opposition to the less heterogeneous microstructures, the highest levels of plasticity are not linked with the porosity where cracks were nucleated. The reason that can explain this fact is that in the FeC and AstMo steels in the surroundings of the cracks, we can find phases/microconstituents with some levels of ductility (ferrite, pearlite, bainite) that could assume the high level of energy that is accumulated in the weakest points. However, here, surrounding the austenite areas, we can find brittle martensite that acts as a fast propagator of the cracks. For DAE, the same brittle behaviour is observed than in the case of AstMo: once the first crack is nucleated, the fracture takes place suddenly. In Ref. 11, where also were performed *in situ* tensile tests, it is concluded that the main path of

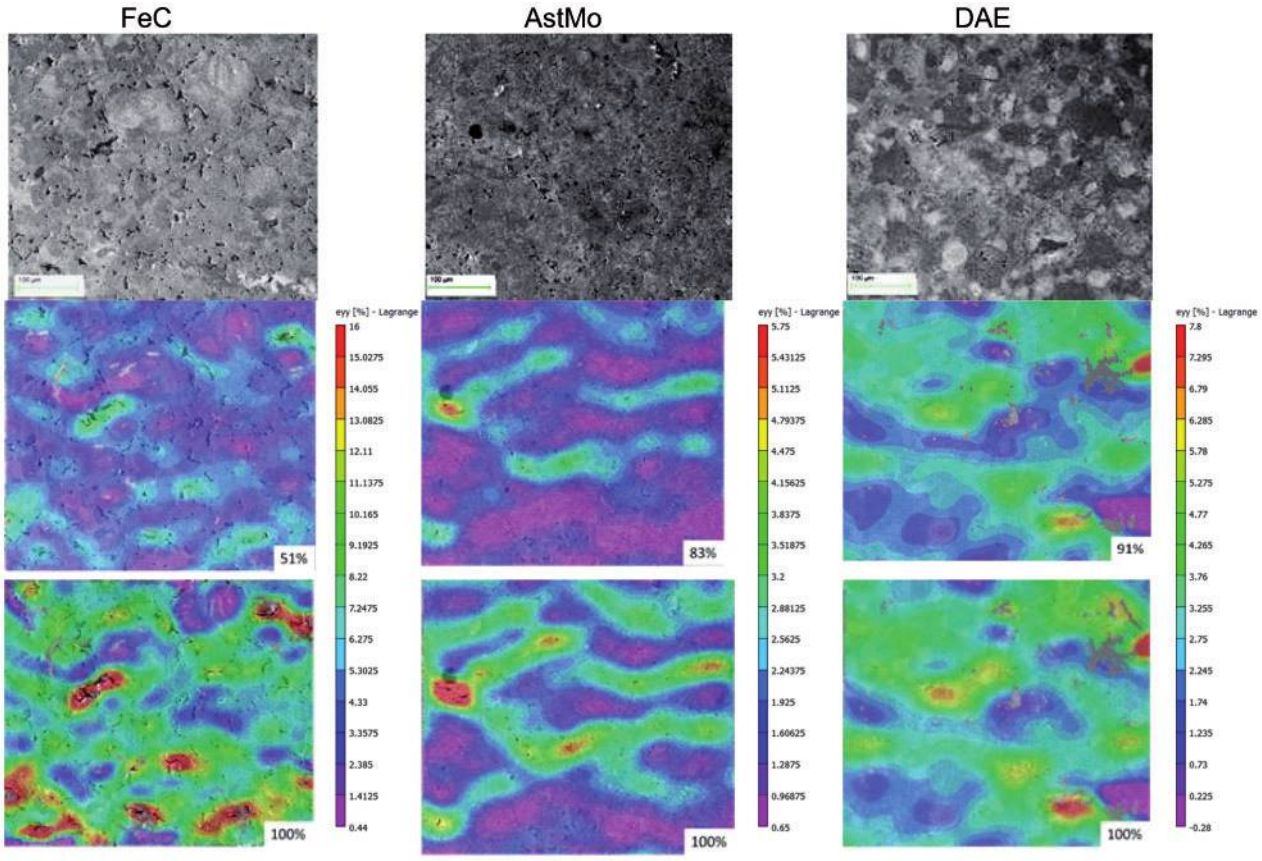

16 **Local deformation maps obtained by DIC technique; scale ε_{yy}=plastic deformation in y axis**

propagation of the fracture is through the ferrite/ferrite interfaces and between the pearlite and the Ni rich ferrite, and to lesser extent, also through the coarse pearlite. In our work, we do not have big areas of ferrite, but the phenomenon that we can confirm is the same preference in the path of the fracture, that is the interfaces between austenite/pearlite, or martensite/pearlite at the sintering necks, and also through the coarse pearlite. Taking into account that big Ni rich areas can promote big porosity, but also can contribute in the absorption of energy in stopping the crack propagation in the places where do not exist pores, if we want to contribute to strength of the steels, the size of those areas should be reduced as much as possible to minimise the negative effect while maintaining its positive contribution to the fracture toughness.

In all the studied families of steels, what can be confirmed with the used techniques is that pores act as stress concentration points to nucleate cracks, and it is clearly seen that the small amount of plasticity that can be generated during the strain of the material is also linked with the places where fracture took place, that is in the neighbouring areas of the pores where cracks nucleate. This is in full accordance with most of the works that have dealt with this matter.[1,4] Finally, in all the studied microstructures, it seems that porosity with it main axis in the perpendicular direction of the applied stress is more damaging in terms of crack nucleation, but this effect has not been fully studied.

Conclusions

From this work, where three different techniques have been combined to analyse the fracture behaviour of four different sintered steels, the following conclusions can be summarised.

1. In all the studied steels, when a tensile load is applied, cracks nucleate in the surrounding of pores, being the sharp pores the most damaging in the process of nucleation of cracks.

2. Once cracks are generated, fracture progresses in a very fast mode in all the studied steels, being the Fe–C steel the one that achieves the highest level of deformation. In all the materials, the fracture is produced very near the formation of the first crack. The material keeps the load until the first crack appears, then propagation is so fast that fracture takes place immediately.

3. In the FeC and AstMo steels, where no martensite is present, the plastic deformation that assumes the strength of the load is located in the neighbouring ductile phases where the crack is generated.

4. In DAE, where some island of Ni rich austenite surrounded by martensite can be found, most of the cracks nucleate in the inherent porosity associated to these areas. Once the cracks have nucleated, they propagate in a very fast manner through the adjacent martensite, between the interface with the pearlite. Here, the plastic deformation during the fracture is assumed by the pearlite.

5. In the developed *in situ* tests, there is no clear evidence of the contribution of the Ni rich areas to the fracture toughness of the studied material. Cracks can be initiated in these areas due to the presence of Kirkendall porosity, but also can be stopped due to the induced transformation from austenite into martensite. Further studies must be carried out to finally clarify the role of the austenitic areas.

Acknowledgement

The authors wish to thank to Höganäs AB for providing all the raw materials to develop this work. The authors also want to thanks to Juan Carlos Rubalcaba for their important contribution in the *''in situ''* tests.

References

1. S. J. Polasik, J. J. Williams and N. Chawla: 'Fatigue crack initiation and propagation in binder-treated powder metallurgy steels', *Metall. Mater. Trans. A*, 2002, **33A**, 73–81.
2. S. Carabajar, C. Verdu, A. Hamel and R. Fougères: 'Fatigue behavior of a nickel alloyed sintered steel', *Mater. Sci. Eng. A*, 1998, **A257**, 225–234.
3. Ch. Xu, H. Danninger, G. Khatibi and B. Weiss: 'Gigacycle fatigue crack initiation in Cr-Mo prealloyed', *Mater. Sci.*, 2007, **534–536**, 685–688.
4. H. Danninger, C. Xu, G. Khatibi, B. Weiss and B. Lindqvist: 'Gigacycle fatigue of ultra high density sintered alloy steels', *Powder Metall.*, 2012, **55**, 378–387.
5. E. Dudrovà and M. Kabátová: 'Fractography of sintered iron and steels', *Powder Metall. Prog.*, 2008, **8**, 59–75.
6. X. Deng, G. Piotrowski, N. Chawla and K. S. Narasimhan: 'Fatigue crack growth behavior of hybrid and prealloyed sintered steels Part I. Microstructure Characterization' *Mater. Sci. Eng. A*, 2008, **A491**, 19–27.
7. A. Piotrowski and G. Biallas: 'Influence of sintering temperature on pore morphology, microstructure, and fatigue behavior of MoNiCu alloyed sintered steel', *Powder Metall.*, 1998, **41**, 109–114.
8. L. Blanco, M. Campos, J. M. Torralba and D. Klint: 'Quantitative evaluation of porosity effects in sintered and heat treated high performance steels', *Powder Metall.*, 2005, **48**, 315–322.
9. N. Chawla and X. Deng: 'Microstructure and mechanical behavior of porous sintered steels', *Mater. Sci. Eng. A*, 2005, **A390**, 98–112.
10. A. Bergmark and L. Alzati: 'Fatigue crack path in Cu-Ni-Mo alloyed PM steel', *Fatigue Fract. Eng. Mater. Struct.*, 2005, **28**, 229–235.
11. X. Deng, G. Piotrowski, N. Chawla and K. S. Narasimhan: 'Fatigue crack growth behavior of hybrid and prealloyed sintered steels. Part II. Fatigue behavior', *Mater. Sci. Eng. A*, 2008, **A491**, 28–38.
12. S. Carabajar, C. Verdu and R. Fougères: 'Damage mechanisms of a nickel alloyed sintered steel during tensile tests', *Mater. Des.*, 1997, **232**, 80–87.
13. M. W. Wu, K. S. Hwang and H. Huang: 'In situ-observations on the fracture mechanism of diffusion alloyed Ni-containing powder metal steels and a proposed method for tensile strength improvement', *Metall. Mater. Trans. A*, 2007, **38A**, 1599–1607.
14. K. P. Mingard and B. Roebuck: 'Mapping complex microstructures in powder metallurgy steels', *Powder Metall.*, 2010, **3**, 191–200.
15. H. Abdoos, H. Khorsand and A. R. Shahani: 'Fatigue behavior of diffusion bonded powder metallurgy steel with heterogeneous microstructure', *Mater. Des.*, 2009, **30**, 1026–1031.
16. R. Cintrón and V. Saouma: 'Strain measurements with the digital image correlation system Vic-2D', CU-NEES-08-06, Center for Fast Hybrid Testing, University of Colorado, Boulder, CO, USA, 2008.
17. B. Tougas, C. Blais, M. Larouche, F. Chagnon and S. Pelletier: 'Characterization of the formation of nickel rich areas in PM nickel steels and their effect on mechanical properties', *Adv. Powder Metall. Part. Mater.*, 2012, **5**, 19–33.